THE ASTROPHYSICAL JOURNAL LETTERS, IN PRESS
Preprint typeset using LaTeX style emulateapj v. 26/01/00

OSSE AND *RXTE* OBSERVATIONS OF GRS 1915+105: EVIDENCE FOR NON-THERMAL COMPTONIZATION

ANDRZEJ A. ZDZIARSKI,[1] J. ERIC GROVE,[2] JURI POUTANEN,[3] A. R. RAO,[4] AND S. V. VADAWALE[4]

The Astrophysical Journal Letters, in press

ABSTRACT

GRS 1915+105 was observed by the *CGRO*/OSSE 9 times in 1995-2000, and 8 of those observations were simultaneous with those by *RXTE*. We present an analysis of all of the OSSE data and of two *RXTE*-OSSE spectra with the lowest and highest X-ray fluxes. The OSSE data show a power-law–like spectrum extending up to $\gtrsim 600$ keV without any break. We interpret this emission as strong evidence for the presence of non-thermal electrons in the source. The broad-band spectra cannot be described by either thermal or bulk-motion Comptonization, whereas they are well described by Comptonization in hybrid thermal/non-thermal plasmas.

Subject headings: accretion, accretion disks — binaries: general — black hole physics — radiation mechanisms: non-thermal — stars: individual (GRS 1915+105) — X-rays: stars

1. INTRODUCTION

The black-hole binary GRS 1915+105 is highly variable in X-rays (Belloni et al. 2000, and references therein). Still, even its hardest spectra are relatively soft, consisting of a blackbody-like component and a high-energy tail (Vilhu et al. 2001). They are softer than those of other black-hole binaries in the hard state, which EF_E spectra peak at ~ 100 keV (e.g., Cyg X-1, Gierliński et al. 1997), and are similar to their soft state (e.g., Cyg X-1, Gierliński et al. 1999, hereafter G99; LMC X-1, LMC X-3, Wilms et al. 2001).

The blackbody component arises, most likely, in an optically-thick accretion disk. On the other hand, there is no consensus at present regarding the origin of the tail. All three main models proposed so far involve Comptonization of the blackbody photons by high-energy electrons. They differ, however, in the distribution (and location) of the electrons, which are assumed to be either thermal (Maxwellian), non-thermal (close to a power law), or in a free fall onto the black hole.

A discussion of these models is given in Zdziarski (2000), who shows that the thermal and free-fall models of the soft state of black hole binaries can be ruled out, mostly by the marked absence of a high-energy cutoff around 100 keV in the *CGRO* data (Grove et al. 1998; G99; Tomsick et al. 1999; McConnell et al. 2000). The present best soft-state model appears to involve electron acceleration out of a Maxwellian distribution (i.e., a non-thermal process), which leads to a hybrid electron distribution consisting of both thermal and non-thermal parts (Zdziarski, Lightman & Maciołek-Niedźwiecki 1993; Poutanen & Coppi 1998; G99; Coppi 1999).

In this *Letter*, we present all OSSE observations of GRS 1915+105. We then choose two OSSE spectra corresponding to the lowest and highest X-ray flux and fit them together with spectra from simultaneous *RXTE* pointed observations. The spectra, showing extended power laws without any cutoff up to at least 600 keV, provide strong evidence for the presence of non-thermal Comptonization. More extensive presentation of the combined X-ray/OSSE data will be given elsewhere.

2. OSSE AND *RXTE* SPECTRA

Table 1 gives the log of the 9 OSSE observations, together with results of power-law fits and basic data about the corresponding X-ray and radio states. The OSSE instrument accumulated spectra in a sequence of 2-min. measurements of the source field alternated with 2-min., offset-pointed measurements of background. The background spectrum for each source field was derived bin-by-bin with a quadratic interpolation in time of the nearest background fields (see Johnson et al. 1993). Figure 1 shows the OSSE spectra (including standard energy-dependent systematic errors), which were fitted up to energies at which the source signal was still detected. The uncertainty for a fitted parameter corresponds hereafter to 90% confidence ($\Delta\chi^2 = 2.71$). We see that the source went through wide ranges of radio and X-ray fluxes and types of X-ray variability during those observations. In spite of that variety, 8 out of 9 OSSE spectra are best-fitted by a power law with a photon index of $\Gamma \simeq 3.0 \pm 0.1$ and the flux varying within a factor of 2. The only exception is the OSSE spectrum corresponding to the highest X-ray flux measured by the ASM (1999 April 21–27), which is much harder, $\Gamma \simeq 2.3$, and has a much lower flux.

We then consider the OSSE spectra corresponding to the extreme X-ray fluxes measured by the *RXTE*/ASM, i.e., from 1997 May 14–20 (VP 619) and 1999 April 21–27 (VP 813). We fit them together with spectra from the pointed *RXTE* observations of 1997 May 15 and 1999 April 23 (the observation IDs are 20187-02-02-00, 40403-01-07-00; 1% systematic error is added to the PCA data with the responses of 2001 February). These PCA data correspond to the variability classes (Belloni et al. 2000) of χ and γ, in which the variability is moderate and the source spends most of the time in two basic low (C) and high (B) X-ray flux state, respectively.

We fit the data with the XSPEC (Arnaud 1996) model `eqpair` (Coppi 1999; G99), which calculates self-consistently microscopic processes in a hot plasma with electron acceleration at a power law rate with an index, $\Gamma_{\rm inj}$, in a background thermal plasma with a Thomson optical depth of ionization

[1]N. Copernicus Astronomical Center, Bartycka 18, 00-716 Warsaw, Poland; aaz@camk.edu.pl
[2]E. O. Hulburt Center for Space Research, Naval Research Laboratory, Washington, DC 20375, USA
[3]Stockholm Observatory, SE-133 36 Saltsjöbaden, Sweden
[4]Tata Institute of Fundamental Research, Homi Bhabha Road, Bombay 400 005, India

electrons, $\tau_{\rm i}$. The electron temperature, kT, is calculated from the balance of Compton and Coulomb energy exchange, as well as $e^{\pm}$ pair production (yielding the total optical depth of $\tau > \tau_{\rm i}$) is taken into account. The last two processes depend on the plasma compactness, $\ell \equiv \mathcal{L}\sigma_{\rm T}/(\mathcal{R}m_{\rm e}c^3)$, where $\mathcal{L}$ is a power supplied to the hot plasma, $\mathcal{R}$ is its characteristic size, and $\sigma_{\rm T}$ is the Thomson cross section. We then define a hard compactness, $\ell_{\rm h}$, corresponding to the power supplied to the electrons, and a soft compactness, $\ell_{\rm s}$, corresponding to the power in soft seed photons irradiating the plasma (which are assumed to be emitted by a blackbody disk with the maximum temperature, $kT_{\rm bb}$). The compactnesses corresponding to the electron acceleration and to a direct heating (i.e., in addition to Coulomb energy exchange with non-thermal $e^{\pm}$ and Compton heating) of the thermal $e^{\pm}$ are denoted as $\ell_{\rm nth}$ and $\ell_{\rm th}$, respectively, and $\ell_{\rm h} = \ell_{\rm nth} + \ell_{\rm th}$. Details of the model are given in G99.

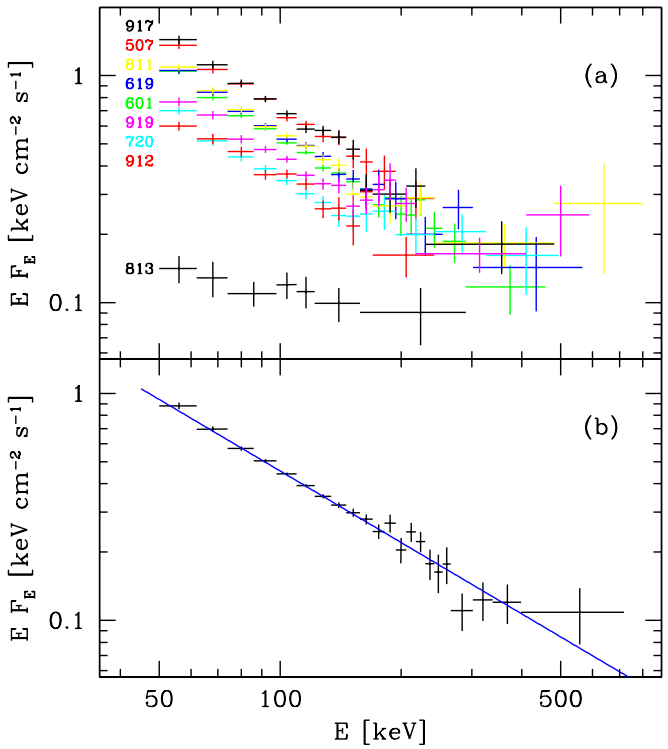

FIG. 1.— (a) The 9 OSSE spectra of GRS 1915+105 deconvolved assuming power-law models. The color-coded spectra are labeled by the OSSE observation numbers (Table 1) ordered according to the 50–60 keV flux. (b) The average spectrum of all observations with its power-law best fit. When fitted by an e-folded power law, the lower limit on the e-folding energy is 0.9 MeV.

We also take into account Compton reflection with a solid angle of Ω (Magdziarz & Zdziarski 1995) and an Fe Kα emission from an accretion disk assumed to extend down to $10GM/c^2$ (which results in a relativistic smearing). The equivalent width, $W_{\rm K\alpha}$, with respect to the *scattered* spectrum only is tied to Ω via $W_{\rm K\alpha} \simeq 100(\Omega/2\pi)$ eV (George & Fabian 1991). The elemental abundances of Anders & Ebihara (1982), an absorbing column of $N_{\rm H} \geq 1.75\times10^{22}$ cm^{-2} (Dickey & Lockman 1990; Vilhu et al. 2001), and an inclination of $i = 70^\circ$ are assumed.

As discussed in G99, χ^2 depends weakly on $\ell_{\rm s}$ in a wide range of this parameter. An increase of $\ell_{\rm s}$ leads to increasing $e^{\pm}$ pair production, which then leads to an annihilation feature around 511 keV. The presence of such a feature is compatible with the OSSE data (Fig. 1), but only very weakly constrained. G99 found that $\ell_{\rm s} = 10$ provides a good fit to Cyg X-1 data. Here, we find that a good fit is provided with $\ell_{\rm s} = 100$, compatible with the high luminosity of GRS 1915+105. For example, for 1/2 of the Eddington luminosity, $L_{\rm E}$, and spherical geometry, the size of the plasma corresponds then to $\sim 100GM/c^2$.

This model provides very good description of our two broadband spectra (as well as of other *RXTE*-OSSE spectra, S. V. Vadawale et al., in preparation). For VP 619, we assume a free relative normalization of the HEXTE and OSSE spectra with respect to those from the PCA. On the other hand, the HEXTE spectrum for VP 813 has relatively few counts at its highest energies, and thus we use the actual OSSE normalization in that fit. Table 2 gives the fit results, and Figure 2 shows the spectra.

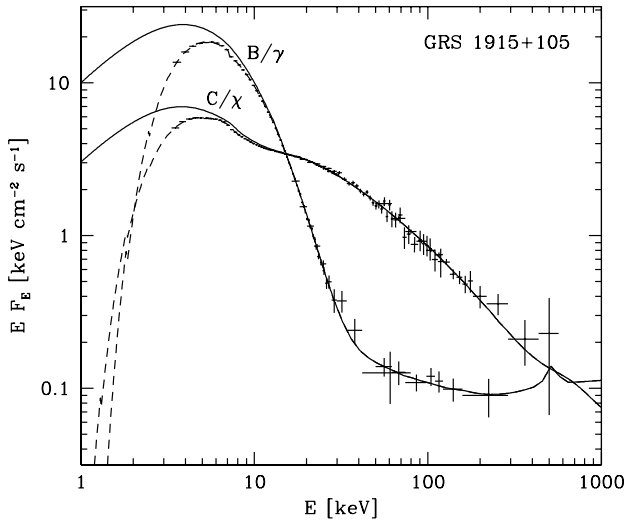

FIG. 2.— Fits to simultaneous PCA-HEXTE-OSSE spectra from VP 619 and 813 with the hybrid Comptonization model. The dashed and solid curves show the models of the observed spectra and the unabsorbed spectra, respectively. The data are normalized to the PCA.

Our model predicts the power law emission extending with no cutoff well above 1 MeV and a weak annihilation feature (with the plasma allowed to be pair-dominated, i.e., with $\tau_{\rm i} \to 0$, for VP 619). Those predictions can be tested by future soft γ-ray detectors more sensitive than the OSSE. We note that the COMPTEL has already detected a power law tail up to $\sim$5–10 MeV in the soft state of Cyg X-1 (McConnell et al. 2000).

Figure 3a shows the spectral components of the fit to the VP-619 spectrum. Compton reflection with $\Omega \sim 2\pi$ is detected at a very high significance ($\Omega = 0$ gives $\chi^2/\nu = 214/131$, corresponding to the chance appearance of reflection of 6×10^{-26} from the F-test), and it is responsible for the convex curvature in the $\sim$10–100 keV spectrum. Figure 3a also shows that the scattered component has a spectral break at ~ 100 keV but continues as a power law (with addition of the broad annihilation feature) above it due to the domination of non-thermal scattering at those energies. Comptonization by the thermal electrons dominates at energies close to the blackbody component and thus PCA data of GRS 1915+105 can be reasonably modeled up to 60 keV by thermal Comptonization of a disk blackbody (Vilhu et al. 2001). When the OSSE data are included, the probability that non-thermal electrons are not present (i.e., $\ell_{\rm nth} = 0$) is only 4×10^{-10}. The best-fit thermal Compton model shown by the long dashes in Figure 3a strongly underestimates the flux above 100 keV. The statistical significance of the presence of non-thermal electrons can be further increased by fitting the *RXTE* spectrum together with the average spectrum from OSSE, which has virtually identical shape to that of VP 619, but much better statistics. Then, allowing for $\ell_{\rm nth} > 0$ reduces χ^2/ν from $228/139$ to $105/137$, which corresponds to

the chance probability of 4×10^{-24}. Thus, we strongly rule out the pure-thermal Comptonization model.

During the VP 813, Compton reflection is statistically not required, as indeed expected at the large $\tau \sim 4$ of the scattering medium covering the disk (which would completely smear out any disk reflection and fluorescence features). Thus, we set $\Omega = 0$ is the fit. The presence of non-thermal electrons is now required at an extremely high significance ($1 - 10^{-40}$) due to the presence of the very distinct hard high-energy tail above the thermally–cut-off spectrum, see Figures 2, 3b.

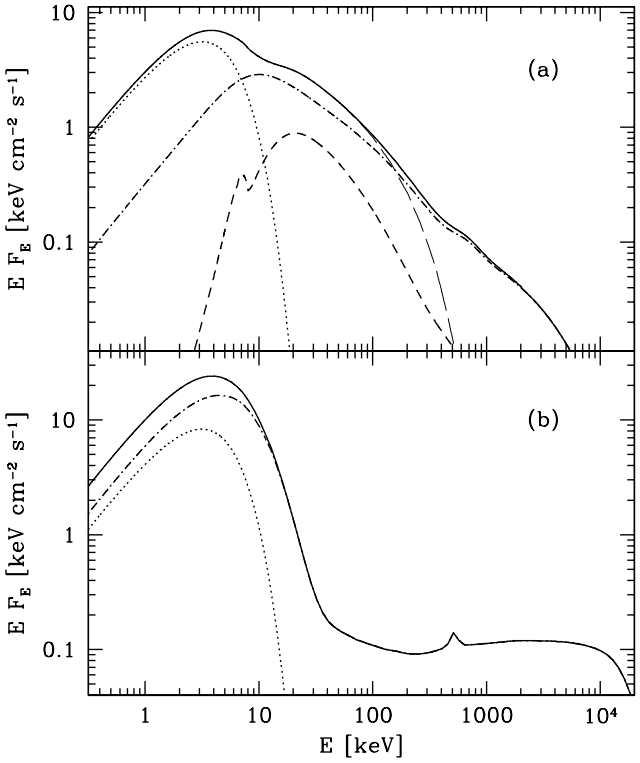

FIG. 3.— (a) Components of the fit to the VP 619 data. All spectra are intrinsic, i.e., corrected for absorption. The dotted, dot-dashed and dashed curves give the unscattered blackbody component, the scattered spectrum, and the component due to Compton reflection and Fe Kα fluorescence, respectively. The solid curve is the total spectrum. The thin long-dashed curve shows the best-fit thermal Comptonization model, which lies much below the data above 100 keV. (b) The total model spectrum and the corresponding two components for the VP 813 data. The cutoff at $\gtrsim 10$ MeV is due to pair absorption.

On the other hand, Shrader & Titarchuk (1998) have fitted a model of bulk-motion Comptonization of blackbody photons to *RXTE* and BATSE data from a hard state of GRS 1915+105 similar to that of VP 619. We fit their model (`bmc` in XSPEC) at a free $N_{\rm H}$ to our broad-band spectra, and find it is completely unacceptable statistically, with $\chi^2/\nu = 851/133$ and $549/92$ for VP 619 and 813, respectively.

However, the *specific* feature of bulk-motion Comptonization is a high-energy cutoff at $\gtrsim 100$ keV due to the effects of Compton recoil and gravitational redshift close to the black-hole horizon (e.g. Laurent & Titarchuk 1999). Such a cutoff is *not* included in the `bmc` model (and its inclusion would further worsen the fits above). Thus, we use Monte Carlo results of Laurent & Titarchuk (1999), which include the cutoff, to test whether the OSSE data (regardless of the data at lower energies) are compatible with its presence. We find that their theoretical spectrum for the accretion rate of $\dot{M} = 2L_{\rm E}/c^2$ matches well the slope of the average OSSE spectrum at low energies (the histogram in Fig. 4). The Monte-Carlo spectrum can then be very well reproduced by a power law times a step function convolved with a Gaussian (model `plabs(step)` in XSPEC, with the cutoff energy of 150 keV and the Gaussian width of 35 keV, the solid curve in Fig. 4). We see that the OSSE average spectrum lies well above that model at $\gtrsim 100$ keV. Quantitatively, the bulk-motion Compton model yields $\chi^2/\nu = 745/48$. In comparison, the power-law and `eqpair` models yield $\chi^2/\nu = 29/48$ and $\chi^2/\nu = 31/44$, respectively. Thus, the bulk-Compton model is completely ruled out. Further problems with that model are discussed in Zdziarski (2000).

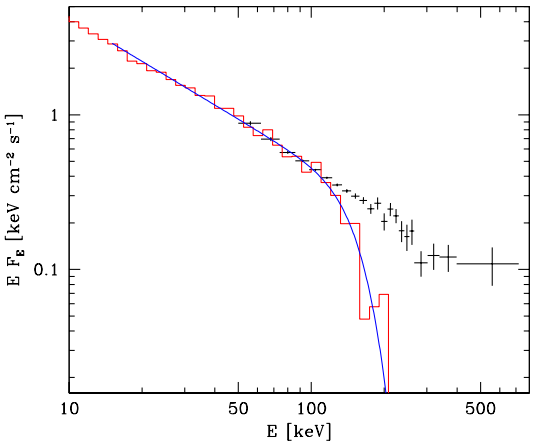

FIG. 4.— Comparison of the average OSSE spectrum fitted by a power law (crosses) with predictions of the bulk-motion Comptonization model (Laurent & Titarchuk 1999; red histogram). The blue solid curve is an analytical approximation of that model, see text. The theoretical spectrum predicts a correct low-energy slope, but it fails to reproduce the data at $\gtrsim 100$ keV.

Also, the commonly used phenomenological models of disk blackbody and either a power law or an e-folded power law give very bad fits to our data. The latter yields $\chi^2/\nu = 263/132$, $405/91$ for VP 619, 813, respectively. In fact, even the thermal part of the VP-813 spectrum is very poorly described by a disk blackbody, with $\chi^2/\nu = 3450/36$ for a fit to the 3.5–20 keV PCA data, whereas the same data are well modeled by thermal Comptonization, $\chi^2/\nu = 22/34$ (with neither model including a high-energy tail). Thus, we find physical models of the spectra of GRS 1915+105 in terms of thermal and non-thermal Comptonization and (in some cases) Compton reflection to be vastly superior to any other model proposed so far.

3. DISCUSSION AND CONCLUSIONS

We have found that broad-band spectra of GRS 1915+105 in its two main spectral states (B, C) are very well fitted by Comptonization of disk blackbody photons in a (hybrid) plasma with both electron heating and acceleration. The presence of strong reflection indicates the plasma is located in coronal regions (possibly magnetic flares) above the disk. This physical model is the same as that fitted to the soft state of Cyg X-1 by G99. Differences in the variability properties of Cyg X-1 and GRS 1915+105 are likely to be due to the disk being stable in the former case and unstable in the latter, most likely due to its much higher $\dot{M}$. The corona is unstable in both cases. The Comptonizing medium in the high-L state (B) is Thomson-thick, and it can represent the surface layer of an overheated disk accreting at a super-Eddington rate (Beloborodov 1998). An issue to be addressed by future research is the origin of the hardening of the tail in this state as compared to other ones (Fig. 1). Our model predicts broad annihilation features, although their strength depends on the unknown size of the plasma.

GRS 1915+105 was in the power-law γ-ray state in the classification of Grove et al. (1998) during the 9 OSSE observations. This state usually corresponds to the high/soft X-ray state. Indeed, X-ray spectra observed so far from GRS 1915+105 (Vilhu et al. 2001) are substantially softer than those with $\Gamma \sim 1.7$ and a sharp thermal cutoff at $E \gtrsim 100$ keV, characteristic to the hard state of other black-hole binaries.

We thank P. Coppi and M. Gierliński for their work on the `eqpair` model, W. N. Johnson for help with the OSSE data reduction, and Ph. Laurent for supplying his Monte Carlo results. This research has been supported by grants from KBN (2P03D00614 and 2P03C00619p1,2), the Foundation for Polish Science (AAZ), and the Swedish Natural Science Research Council and the Anna-Greta and Holger Crafoord Fund (JP). JP and AAZ acknowledge support from the Royal Swedish Academy of Sciences, the Polish Academy of Sciences and the Indian National Science Academy through exchange programs.

REFERENCES

Anders, E., & Ebihara, M. 1982, Geochim. Cosmochim. Acta, 46, 2363
Arnaud, K. A. 1996, in ASP Conf. Series 101, Astronomical Data Analysis Software and Systems V, ed. G. H. Jacoby & J. Barnes (San Francisco: ASP), 17
Belloni, T., Klein-Wolt, M., Méndez, M., van der Klis, M., & van Paradijs, J. 2000, A&A, 355, 271
Beloborodov, A. M. 1998, MNRAS, 297, 739
Coppi, P. S. 1999, in ASP Conf. Ser. Vol. 161, High Energy Processes in Accreting Black Holes, eds. J. Poutanen & R. Svensson (San Francisco: ASP), 375
Dickey, J., & Lockman, F. 1990, ARA&A, 28, 215
George, I. M., & Fabian, A. C. 1991, MNRAS, 249, 352
Gierliński, M., Zdziarski, A. A., Done, C., Johnson, W. N., Ebisawa, K., Ueda, Y., Haardt, F., & Phlips, B. F. 1997, MNRAS, 288, 958
Gierliński, M., Zdziarski, A. A., Poutanen, J., Coppi, P. S., Ebisawa, K., & Johnson, W. N. 1999, MNRAS, 309, 496 (G99)
Grove, J. E., Johnson, W. N., Kroeger, R. A., McNaron-Brown, K., & Skibo, J. G. 1998, ApJ, 500, 899
Johnson, W. N., et al. 1993, ApJS, 86, 693
Laurent, P., & Titarchuk, L. 1999, ApJ, 511, 289
Magdziarz, P., & Zdziarski, A. A. 1995, MNRAS, 273, 837
McConnell, M. L., et al. 2000, in McConnell M. L., Ryan J. M., eds., AIP Conf. Proc. 510, The Fifth Compton Symposium. Melville, New York, 114
Poutanen, J., & Coppi, P. S. 1998, Physica Scripta, T77, 57
Shrader, C., & Titarchuk, L. 1998, ApJ, 499, L31
Tomsick, J. A., Kaaret, P., Kroeger, R. A., & Remillard, R. A. 1999, ApJ, 512, 892
Vilhu, O., Poutanen, J., Nikula, P., & Nevalainen, J. 2001, ApJL, in press (astro-ph/0010601)
Wilms, J., Nowak, M. A., Pottschmidt, K., Heindl, W. A., Dove, J. B., & Begelman, M. C. 2001, MNRAS, 320, 327
Zdziarski, A. A. 2000, in IAU Symp. 195, Highly Energetic Physical Processes and Mechanisms for Emission from Astrophysical Plasmas, ed. P. C. H. Martens, S. Tsuruta & M. A. Weber (San Francisco: ASP), 153 (astro-ph/0001078)
Zdziarski, A. A., Lightman, A. P., & Maciołek-Niedźwiecki, A. 1993, ApJ, 414, L93

TABLE 1
OSSE OBSERVATIONS OF GRS 1915+105

OSSE VP[a]	Start date	End date	Exposure[b] [10^5 s]	Γ	OSSE flux[c]	X-ray obs.[d]	X-ray flux[e] [mCrab]	2.2 GHz flux [mJy]
507	1995 Nov 28	Dec 7	2.26	$3.08^{+0.08}_{-0.07}$	$18.8^{+0.5}_{-0.4}$			
601	1996 Oct 15	Oct 29	7.15	$3.08^{+0.05}_{-0.05}$	$14.1^{+0.2}_{-0.2}$	$\nu\chi\chi\nu\chi$	840±330[f]	
619	1997 May 14	May 20	3.27	$3.06^{+0.06}_{-0.06}$	$14.7^{+0.3}_{-0.4}$	$\alpha\chi\chi\alpha\chi$	270±120	33±12[f]
720	1998 May 5	May 15	4.20	$3.00^{+0.09}_{-0.09}$	$9.5^{+0.3}_{-0.2}$	$\chi\chi\chi\chi\chi$	570±40	91±22
811	1999 Apr 6	Apr 13	2.92	$3.10^{+0.07}_{-0.07}$	$14.9^{+0.3}_{-0.4}$	$\alpha\rho\rho$	830±350	11±6
812	1999 Apr 14	Apr 20	2.85	$2.89^{+0.10}_{-0.10}$	$9.5^{+0.4}_{-0.3}$	$\kappa\kappa\kappa\kappa\kappa\kappa$	920±270	9±4
813	1999 Apr 21	Apr 27	3.23	$2.33^{+0.28}_{-0.27}$	$3.0^{+0.4}_{-0.3}$	γ	1190±240	10±4
917	2000 Apr 18	Apr 25	1.56	$3.16^{+0.08}_{-0.07}$	$19.1^{+0.4}_{-0.4}$	$\chi\chi\chi\chi\alpha\alpha$	430±100	19±7
919	2000 May 9	May 26	3.89	$2.96^{+0.08}_{-0.08}$	$11.5^{+0.3}_{-0.3}$	$\chi\rho\rho\rho\rho\rho\rho\rho\rho$	700±90	
Sum			29.60	$3.05^{+0.04}_{-0.04}$	$12.2^{+0.1}_{-0.2}$			

[a] *CGRO* Viewing Period.
[b] Scaled to a single OSSE detector.
[c] For 50–300 keV in units of 10^{-10} erg cm^{-2} s^{-1}.
[d] Pointed *RXTE* observations with Greek letters giving their variability in the classification of Belloni et al. (2000).
[e] The *RXTE*/ASM 2–12 keV flux.
[f] These errors give the standard deviation of the flux variability.

TABLE 2
MODEL PARAMETERS OF THE BROAD-BAND SPECTRA

OSSE VP	$N_{\rm H}$ [10^{22} cm^{-2}]	$kT_{\rm bb}$ [keV]	$\ell_{\rm h}/\ell_{\rm s}$	$\ell_{\rm nth}/\ell_{\rm h}$	$\Gamma_{\rm inj}$	$\tau_{\rm i}$	τ[a]	kT[a] [keV]	$\Omega/2\pi$	$F_{\rm bol}$[b]	$L_{\rm iso}$[c]	χ^2/ν[d]
619	$3.2^{+0.3}_{-0.4}$	$1.37^{+0.05}_{-0.05}$	$0.48^{+0.03}_{-0.03}$	$0.23^{+0.31}_{-0.13}$	$3.0^{+0.8}_{-0.6}$	$0.26^{+0.34}_{-0.26}$	0.39	66	$0.96^{+0.50}_{-0.26}$	3.5	6.5	91/130
813	$6.1^{+0.5}_{-0.4}$	$1.35^{+0.04}_{-0.02}$	$0.29^{+0.02}_{-0.01}$	$0.12^{+0.02}_{-0.01}$	$2.2^{+0.2}_{-0.2}$	$4.42^{+0.14}_{-0.06}$	4.43	3.6	0 (fixed)	8.9	17	60/90

[a] The total optical depth and the electron temperature calculated from energy and pair balance for the best-fit model (i.e., not free parameters).
[b] The unabsorbed bolometric flux of the model in units of 10^{-8} erg cm^{-2} s^{-1}.
[c] The model luminosity assuming isotropy and a distance of 12.5 kpc in units of 10^{38} erg s^{-1}.
[d] The values of $\chi^2/\nu < 1$ result here from the assumed systematic errors, and are not due to overmodeling.